

ornl

ORNL/TM-11053

**OAK RIDGE
NATIONAL
LABORATORY**

MARTIN MARIETTA

**A Study of the
Tribological and Surface
Micromechanical Properties
of $\text{YBa}_2\text{Cu}_3\text{O}_{7-x}$**

Final Report

P. J. Blau
C. E. DeVore
D. F. Wilson
J. R. Keiser

OAK RIDGE NATIONAL LABORATORY
CENTRAL RESEARCH LIBRARY
CIRCULATION SECTION
4590N ROOM 173

LIBRARY LOAN COPY

DO NOT TRANSFER TO ANOTHER PERSON

If you wish someone else to see this
report, send in name with report and
the library will arrange a loan.

OPERATED BY
MARTIN MARIETTA ENERGY SYSTEMS, INC.
FOR THE UNITED STATES
DEPARTMENT OF ENERGY

This report has been reproduced directly from the best available copy.

Available to DOE and DOE contractors from the Office of Scientific and Technical Information, P.O. Box 62, Oak Ridge, TN 37831; prices available from (615) 576-8401, FTS 626-8401.

Available to the public from the National Technical Information Service, U.S. Department of Commerce, 5285 Port Royal Rd., Springfield, VA 22161.

NTIS price codes—Printed Copy: A04 Microfiche A01

This report was prepared as an account of work sponsored by an agency of the United States Government. Neither the United States Government nor any agency thereof, nor any of their employees, makes any warranty, express or implied, or assumes any legal liability or responsibility for the accuracy, completeness, or usefulness of any information, apparatus, product, or process disclosed, or represents that its use would not infringe privately owned rights. Reference herein to any specific commercial product, process, or service by trade name, trademark, manufacturer, or otherwise, does not necessarily constitute or imply its endorsement, recommendation, or favoring by the United States Government or any agency thereof. The views and opinions of authors expressed herein do not necessarily state or reflect those of the United States Government or any agency thereof.

Metals and Ceramics Division

A STUDY OF THE
TRIBOLOGICAL AND SURFACE MICROMECHANICAL PROPERTIES
OF $\text{YBa}_2\text{Cu}_3\text{O}_{7-x}$

FINAL REPORT

P. J. Blau, C. E. DeVore, D. F. Wilson, and J. R. Keiser

Date Published - July 1989

Prepared for
Argonne National Laboratory
Argonne, IL 60439
and
the Assistant Secretary for
Conservation and Renewable Energy,
Office of Energy Utilization Research,
Energy Conversion and Utilization Technologies
(ECUT) Tribology Program
(EG 05 00 00 0)

Prepared by the
OAK RIDGE NATIONAL LABORATORY
Oak Ridge, TN 37831-6285
operated by
MARTIN MARIETTA ENERGY SYSTEMS, INC.
for the
U.S. DEPARTMENT OF ENERGY
under contract DE-AC05-84OR21400



FOREWORD

This one-year survey of superconductor tribology was sponsored by Argonne National Laboratory in conjunction with the U.S. Department of Energy, Energy Conversion and Utilization Technologies (ECUT) Tribology Project (Dr. Fred A. Nichols, ANL, Project Manager). The purpose of this investigation was to develop background data on the friction and wear-related properties of a typical high-temperature superconducting oxide ceramic. At the time this project was initiated, the emphasis was directed at $\text{YBa}_2\text{Cu}_3\text{O}_{7-x}$; however, since that time, other oxide ceramics with attractive high-temperature superconducting properties have been discovered. Since most of these materials exhibit similar brittle behavior, portions of the current study on $\text{YBa}_2\text{Cu}_3\text{O}_{7-x}$ may be at least qualitatively descriptive of the surface damage which may be experienced by sliding or abrasive contact of other superconducting materials. The intent of this study is to serve as a baseline for evaluating potential problems in handling and using such materials in applications involving direct surface contact.



CONTENTS

FOREWORD	iii
LIST OF FIGURES	vii
LIST OF TABLES	ix
ABSTRACT	1
1. INTRODUCTION	2
2. MATERIALS	6
3. EXPERIMENTAL METHODS AND RESULTS	7
3.1. MICROINDENTATION HARDNESS TESTS	7
3.2. NANOINDENTATION EXPERIMENTS	10
3.3. SCRATCH HARDNESS TESTING	14
3.4. ABRASION EXPERIMENT	16
3.5. RECIPROCATING SLIDING FRICTION AND WEAR TESTS	19
3.6. UNIDIRECTIONAL SLIDING FRICTION AND WEAR TESTS	27
4. SUMMARY AND CONCLUSIONS	32
ACKNOWLEDGMENTS	34
REFERENCES	34

LIST OF FIGURES

<p>Fig. 1. Subject areas covered by presentations at the American Ceramic Society Meeting (April 1987) and the Materials Research Society Meeting (November 1987)</p>	3
<p>Fig. 2. Cross section of a plasma-sprayed 1-2-3 on stainless steel specimen showing the irregular microstructure of the coating and the heat-affected zone in the substrate</p>	8
<p>Fig. 3. Single crystal of 1-2-3 compound before (left) and after (right) microindentation testing</p>	9
<p>Fig. 4. Schematic diagram of the Nanoindenter™</p>	11
<p>Fig. 5. Typical raw data for sensor voltages used to construct a load-displacement curve for an individual indentation experiment on 1-2-3</p>	12
<p>Fig. 6. Pattern of triangular indentations extending across several grain boundaries in a Brynstad specimen which was 93% dense</p>	13
<p>Fig. 7. Diagram of the scratch tester used in this study</p>	14
<p>Fig. 8. Comparison of scratch testing data for 1-2-3 and several pure metals showing a decline in scratch hardness numbers (SHN) with increasing load</p>	16
<p>Fig. 9. Scratch damage to the rod material at 25-g (left) and 100-g (right) stylus loads (original mag. 500X)</p>	17
<p>Fig. 10. Area of an abraded specimen showing long grooves (horizontal) characteristic of abrasion (scanning electron micrograph)</p>	19
<p>Fig. 11. Higher magnification scanning electron micrograph of a single groove showing ductile tearing in the groove and brittle fracture beside it</p>	20
<p>Fig. 12. Diagram of the reciprocating friction testing apparatus and the slider holder arrangement</p>	21
<p>Fig. 13. Slider configurations for sliding friction and wear tests</p>	22
<p>Fig. 14. Friction coefficient vs log sliding cycles for tests at 1.96 N load</p>	23
<p>Fig. 15. Friction coefficient vs log sliding cycles for tests at 0.98 N load</p>	24

Fig. 16. Gold-filled pores on the sliding surface of the Brynestad material (original mag. 500X)	25
Fig. 17. Dark transfer film, possibly friction polymer, on the tip of the gold slider (original mag. 500X)	26
Fig. 18. Needle-like debris caught in a pore on the sliding surface from a self-mated test	28
Fig. 19. Microstructure of commercially prepared 1-2-3. The quality of this polyphase material was inferior to that of the Argonne materials in that the disks were often found to contain hairline cracks running across them. They had to be handled carefully during polishing and testing to make sure they did not fracture	29
Fig. 20. Schematic diagram of the pin-on-disk tribometer used for unidirectional sliding experiments. The friction force sensing arrangement was similar to that in Fig. 12	30
Fig. 21. Scanning electron micrograph of pulverized debris covering the wear track. Sizes ranged from less than 1 μm to several micrometers	32
Fig. 22. Scanning electron micrograph showing that once debris compacts formed, they could shear plastically	33

LIST OF TABLES

Table 1. Sources and materials used in this study (all materials were $\text{YBa}_2\text{Cu}_3\text{O}_{7-x}$) 6

Table 2. Knoop microindentation hardness of $\text{YBa}_2\text{Cu}_3\text{O}_{7-x}$ specimens 10

Table 3. Nanoindentation properties of $\text{YBa}_2\text{Cu}_3\text{O}_{7-x}$ (25 values per material recorded at a penetration depth of 200 nm) 13

Table 4. Unidirectional sliding friction and wear of $\text{YBa}_2\text{Cu}_3\text{O}_{7-x}$ 31

A STUDY OF THE TRIBOLOGICAL AND SURFACE
MICROMECHANICAL PROPERTIES OF $\text{YBa}_2\text{Cu}_3\text{O}_{7-x}$ *

P. J. Blau, C. E. DeVore, D. F. Wilson, and J. R. Keiser

ABSTRACT

The burgeoning interest in high critical temperature (T_c) superconductors has created a need to examine the technological properties of these materials for the purpose of defining potential applications and handling characteristics. While new superconducting compounds continue to be developed, the perovskite-structure oxide ceramics form the basis for these new materials. This report discusses information obtained about the reciprocating sliding friction coefficients (self-mated and on gold), scratch resistance, microindentation hardness, and wear damage mechanisms in $\text{YBa}_2\text{Cu}_3\text{O}_{7-x}$ compounds fabricated in several ways. As expected, the materials are quite brittle. Knoop microindentation hardness numbers for single crystals can exceed 4.41 GPa (450 kg/mm²). Low-load, precision indentation experiments provided information on the hardness of thin surface regions less than 300 nm deep, as well as on the modulus of elasticity. The modulus of elasticity obtained by indentation experiments was 78 to 81 GPa, which is in relatively good agreement with density-corrected published values obtained by ultrasonic methods. Scratch resistance using a diamond stylus test falls with increasing load because both intergranular and transgranular cracking increase with load. The abrasion rate of $\text{YBa}_2\text{Cu}_3\text{O}_{7-x}$ on 180-grit silicon carbide papers is linearly proportional to normal load. Friction coefficients on gold range from 0.12 to 1.0 depending on test duration, and those for self-mated sliding range between 0.15 and 1.1, also depending on test duration. Unlubricated friction coefficients for $\text{YBa}_2\text{Cu}_3\text{O}_{7-x}$ are too high for most potential tribological applications. Wear coefficients for pin-on-disk tests give values in the severe wear range. Overall results confirm that the $\text{YBa}_2\text{Cu}_3\text{O}_{7-x}$ materials are brittle in their monolithic form, and their use in tribological applications should be avoided unless a suitable, more damage-tolerant composite can be developed.

*Research sponsored by the Office of Energy Utilization Research, Energy Conversion and Utilization Technologies (ECUT) Program, U.S. Department of Energy, under contract DE-AC05-84OR21400 with Martin Marietta Energy Systems, Inc.

1. INTRODUCTION

The discovery of a class of relatively high critical temperature superconducting ceramic oxides (HTSC) by Müller and Bednorz¹ had such a profound potential impact on science and technology that they were awarded the Nobel Prize in Physics less than 2 years after the discovery.² Both the technical literature and the popular science magazines have been deluged with hundreds of review articles and research papers on the HTSC materials. In January 1988, three magazines, *Science*, *American Scientist*, and *Advanced Materials and Processes*, all featured the structure of the Y-Ba-Cu-O compound on their front covers, and numerous other journals have followed suit. Economic and technological consequences of the discovery have also been discussed at length.³⁻⁷ Some articles discuss the tremendous potential of these materials, while others discuss their impact on U.S. competitiveness on the world market. Several on-line computer databases and abstracting services have quickly been developed. Notable among these is the Department of Energy's Superconductivity Information System (SIS) developed for the Office of Scientific and Technical Information (OSTI) by Science Applications International Corporation.

The topics of greatest interest in HTSC research were surveyed by separating the papers presented at two recent technical society meetings into nine topical areas:

1. chemical or moisture effects on HTSC materials;
2. crystal structure determinations;
3. microstructural characterization and microscopy other than that involved in item 2 (grain structure, twinning, grain boundary structure);
4. mechanical properties;
5. physical properties such as thermal conductivity, electrical conductivity, heat capacity, magnetic properties (other than the Meissner effect), optical properties, and ultrasonic energy transmission behavior;
6. quantum theory and superconductivity theory;

7. processing and fabrication;
8. Meissner effect; and
9. other, including thermodynamics, irradiation effects, stoichiometry effects on T_c , and areas not covered above.

The two meetings surveyed were the 1987 Fall Meeting of the Materials Research Society (November) and the 89th Annual Meeting of the American Ceramic Society (April 1987). The former meeting had 233 papers on HTSC and the latter 50. Figure 1 shows the distribution of topics based on the titles of the papers. It is quite clear that processing and fabrication of the materials dominated the work presented at these two meetings. Numerous ways of processing the materials are being developed, but relatively little work is being done on characterizing their mechanical properties. An on-line search of the aforementioned OSTI (SIS) database in early January 1988

ORNL-DWG 88-9295

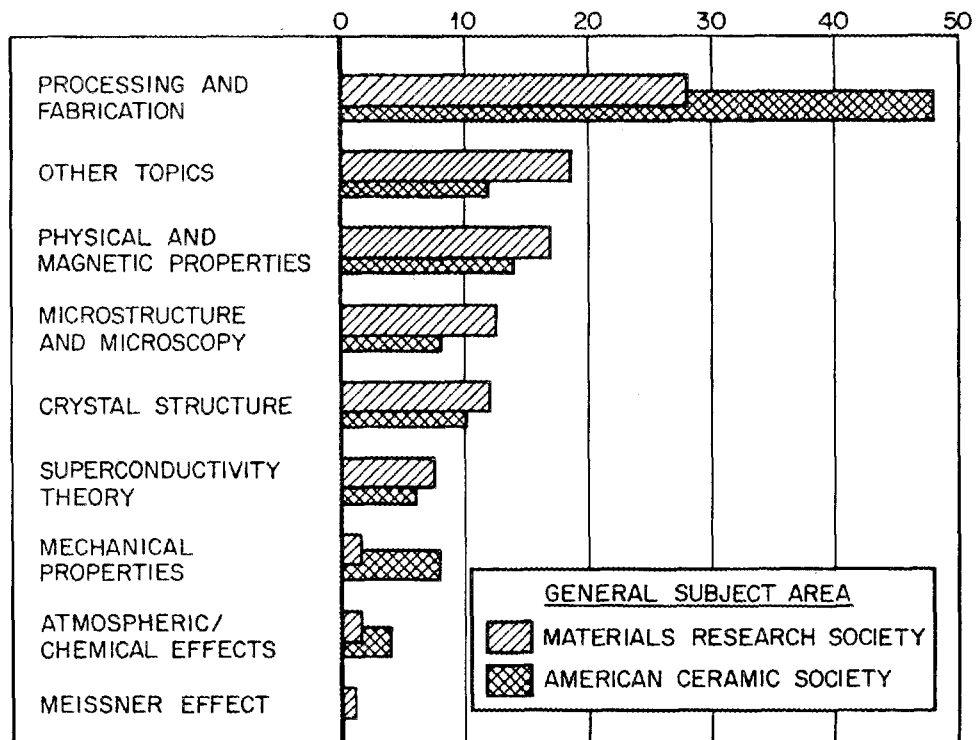


Fig. 1. Subject areas covered by presentations at the American Ceramic Society Meeting (April 1987) and the Materials Research Society Meeting (November 1987).

turned up very few studies of the mechanical properties of the HTSC and nothing whatsoever about their friction and wear. Furthermore, a study of the collected papers from *Physical Review Letters* and *Physical Review B* from January through June 1987 revealed that only one paper⁸ dealt with mechanical properties (the elastic modulus of $\text{La}_{2-x}\text{Sr}_x\text{CuO}_4$).

Young's modulus, the shear modulus, and Poisson's ratio measure materials properties that affect the contact stress, and hence affect the friction and wear. Several research papers have attempted to measure such properties in Y-Ba-Cu-O materials. Ledbetter et al.⁹ estimated the elastic constants for the fully dense condition of $\text{YBa}_2\text{Cu}_3\text{O}_{7-x}$ (hereafter called "1-2-3") using corrections to values obtained by ultrasonic techniques applied to porous (30.5% void content) sintered disk specimens. They reported a shear modulus of 35 to 42.5 GPa, a Young's modulus of 90.8 to 101.8 GPa, and a Poisson's ratio of 0.198 to 0.290 after density corrections. In a subsequent paper, Ledbetter et al.¹⁰ described an apparent discontinuous increase in the shear modulus below 65 K; the reasons offered for this were either strong electronic changes that decreased the crystal volume or a crystal structure change. From the indentation data of Cook et al.,¹¹ a calculated value of 350 GPa parallel to the c-axis could be obtained, but this was based on the assumption that the ratio of Young's modulus to hardness (E/H) for the material was 40. This 350-GPa value for E is much higher than that obtained by Ledbetter et al. Furthermore, Chang et al.¹² used a Hertzian sphere indentation technique to obtain a Young's modulus of 226 GPa, a Poisson's ratio of 0.30, and a derived shear modulus of 87 GPa. Tests were done on materials with porosities of 17, 23, and 35% so that the calculated Young's modulus could be corrected for porosity effects.

Work also has been conducted on the effects of pressure on the critical superconducting transition temperature. Since rubbing contacts involve compressive and shear stresses, any degradation in superconducting properties due to surface contact could be important. Erskin et al.¹³ described the pressure dependence of copper oxide-based La-Sr superconductors at applied pressures of over 8 GPa using a diamond anvil cell on 200- μm -sized pellets made by crushing 78% dense compacts. The opposing diamond platens impose a "quasi-hydrostatic" stress field on the material

by having the specimen surrounded with soft powder. At about 5 GPa, the T_c reached a maximum of about 46 K. However, above 8 GPa, the T_c markedly decreased, and at 9 GPa, it disappeared completely. Furthermore, the room temperature conductivity of the 8 GPa-compressed sample decreased by an order of magnitude even though it had lost much of its low-temperature superconductivity. The implication is that higher bearing pressures may degrade superconductivity; however, more experiments are needed in this area, especially with 1-2-3 and other compounds of more recent interest.

Park et al.¹⁴ have investigated the effects of tensile and compressional strains on T_c in 1-2-3. They found that the T_c increases linearly with compressional strain, but also found that T_c is only slightly (~ 0.3 K) reduced under tensile strains. This reported increase in T_c in the 1-2-3 compound is the reverse of the decreasing T_c observed in the high pressure experiments with the La-Sr-Cu-O compounds described earlier. Clearly, work is needed in the area of contact stress effects on superconductor performance if any electrical connector, relay, or motor brush applications are of interest.

The current study was conducted as a contribution to the technology base for the fabrication and application of superconducting ceramic oxides. Fabrication techniques involving mechanical working, and applications such as electrical contacts in connectors and relays and in motor brushes may benefit from a knowledge of the friction and wear characteristics of HTSC. While research continues to push the T_c higher and higher (recent, unconfirmed results from Taiwanese investigators indicate T_c as high as 162 K for a "four-layered" Tl-Ca-Ba-Cu-O compound¹⁵), this study initially identified 1-2-3 as the material of study. Specimen materials of 1-2-3 compound have been obtained from five sources in several forms and densities so that a broader survey of friction and wear-related properties could be performed. This report presents the results and discusses the findings of a one-year survey of tribological properties of 1-2-3. The data reported here include microindentation hardness, low-penetration "nanohardness," scratch testing, abrasion testing, and sliding friction and wear.

2. MATERIALS

The sources and descriptions of the materials used in this study are given in Table 1. Specimens of different types required different methods of preparation for hardness, friction, and wear studies. When flat specimens were involved, they were mechanically polished, finishing with a

Table 1. Sources and materials used in this study
(all materials were $\text{YBa}_2\text{Cu}_3\text{O}_{7-x}$)

-
1. J. Brynstad (ORNL, Chemistry Division)
Mounted and polished portions of 4.0-mm-diam cylindrical pellets produced as follows: weigh and mix powders of barium carbonate, yttrium oxide, and copper oxide in a helium-atmosphere dry box; press into pellets and calcine at 900°C for 16 to 24 h in oxygen; regrind and repeat process three times at successively increasing temperatures ending with 950°C; and slow cool in oxygen with several hour holds at 550 and 400°C. Final densities of the samples were between 93 and 94% of theoretical density. Grains were angular and blocky (3.0 to 6.0 μm ; typical aspect ratios 1 to 2.5).
 2. R. B. Poeppel and K. C. Goretta (Argonne National Laboratory)
Sintered disks 2.0 cm in diameter and 0.8 cm thick. Prepared using a nitrite precursor, average grain size 0.15 μm . Cold-pressed without binder in a 2.54-cm-diam die, placed on MgO, and fired in flowing O_2 as follows: heat at 300°C/h to 980°C, hold 4 h, cool to 520°C in 1.5 h, cool to 390°C in 16 h, then cool in about 4 h to room temperature. The final density was about 98% of theoretical. Grains were rectangular in cross section (aspect ratios 6 to 15). Duplex grain size: small ones 2 to 4 μm across, and large, elongated ones with some over 100 μm long.
 3. L. Boatner (ORNL, Solid State Division)
Loose single crystal platelets grown by a hot solution flux technique. The c-axis of the crystals was normal to the platelet flat surface, and the unfractured edges of the crystals were parallel to the a- and b-axes. Crystals averaged about 1 or 2 mm on a side and less than 0.1 mm thick. They were quite fragile.
 4. Lambertville Ceramic Manufacturing Company, Lambertville, N.J.
Sintered and fired polycrystalline disks. High temperature firing produced what the manufacturer called "high-fire, fully dense" material. The apparent density was, however, 5.171 g/cm³, and the microstructure appeared to be polyphase. (See photomicrograph in Fig. 19.)
-

vibratory slurry technique. The preparation of hemispherical specimens used for wear tests is described in the section on friction and wear testing. Because of their potential sensitivity to moisture, porous powder compacts were stored in a desiccator when not being tested or examined. In the experience of the current investigators, there was no apparent effect of laboratory air exposure on the repeatability of friction or wear experiments, and no evidence of microstructural deterioration was evident upon reexamination of polished surfaces more than six months after preparation.

Plasma-sprayed 1-2-3 materials were obtained from Idaho National Engineering Laboratory (INEL). Cross sections were prepared to determine whether friction and wear testing would be feasible on the coupons. The photomicrograph in Fig. 2 reveals their irregular microstructures and rough surfaces. The heat-affected zone caused by plasma spraying could be observed in the stainless steel substrate. The form of this material did not allow either scratch testing or tribotesting to be satisfactorily performed.

The availability of prepared 1-2-3 materials for use in this survey greatly improved during the course of the work, and the last series of experiments were performed with commercially prepared materials.

3. EXPERIMENTAL METHODS AND RESULTS

The experimental techniques used in this investigation were: micro-indentation hardness testing, nanoindentation testing, scratch tests, dry sliding abrasion tests, and sliding friction and wear tests, both reciprocating and unidirectional. Each is described in a separate section.

3.1. MICROINDENTATION HARDNESS TESTS

The Knoop microindentation tests were performed on a bench-top commercial instrument (Shimadzu Type M). While low loads were used to minimize indentation-induced fracture, some evidence of microfracture was observed with most of the indentations.

Microindentation hardness data were obtained on the specimens provided by J. Brynestad of Oak Ridge National Laboratory (ORNL) and on a disk

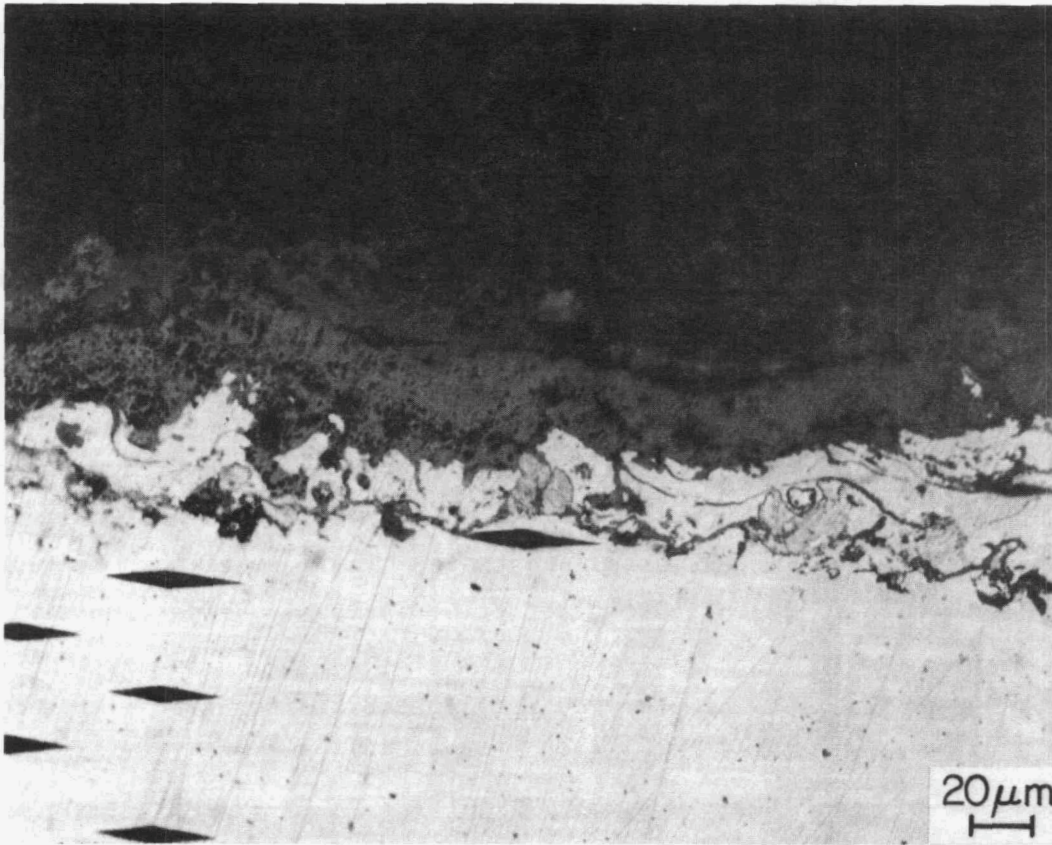


Fig. 2. Cross section of a plasma-sprayed 1-2-3 on stainless steel specimen showing the irregular microstructure of the coating and the heat-affected zone in the substrate.

specimen provided by R. B. Poeppel of Argonne National Laboratory (ANL). The grain size of the polycrystalline specimens from Brynestad permitted indentations to be made in individual grains at loads up to 0.98 N; however, the ANL specimens had smaller, more slender grains, and most indentations crossed at least one grain boundary. Nearly all indentations produced fine, brittle cracks. Because of the uncertainties inherent when testing porous, brittle compacts, the higher hardness values are more likely to be representative of the material than the lower ones, which could have been influenced by either microcracking or by a lack of subsurface mechanical support for the indented volume. Despite the

differences in grain structure and method of fabrication, the average Knoop microindentation hardnesses of ORNL and ANL compacts were comparable.

Knoop microindentations were also made on the thin, delicate single crystals provided by L. Boatner of ORNL. The crystals were about 1-2 mm across and <0.2 mm thick. The test surfaces were perpendicular to the c-axis in the solution-grown crystals. Uncracked, readable impressions were obtained with difficulty only at applied loads of 0.15 and 0.25 N. They were made selectively on areas of the crystals which appeared flat in the optical microscope at 400X. In several cases, the indentation process resulted in fractures of the crystals. These fractures mainly paralleled the "a" and "b" directions in the (001) surface of the crystal (Fig. 3). The microindentation hardness numbers obtained on the single crystals were higher than those obtained on individual grains of the sintered compact from J. Brynestad. These data are given in Table 2. The average values for the sintered materials at the 0.25-N indentation load was 2.8 GPa compared with 4.1 GPa for the two single crystals. The data previously reported by Blendell et al.¹⁸ for sintered powder was 3.7 ± 0.5 GPa, and limited data from Livingston et al.¹⁶ at 25 g load ranged from 4.9 GPa [parallel to the (001) plane] to 9.4 GPa [perpendicular to the (001) plane].

ORNL-PHOTO 2438-89

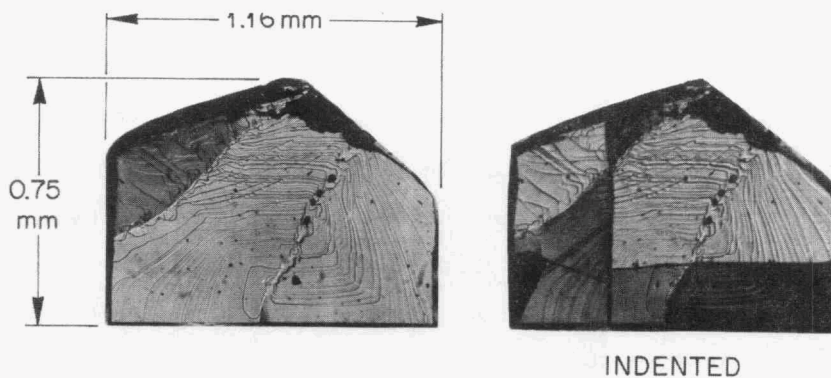


Fig. 3. Single crystal of 1-2-3 compound before (left) and after (right) microindentation testing.

Table 2. Knoop microindentation hardness of $\text{YBa}_2\text{Cu}_3\text{O}_{7-x}$ specimens

Source	Form	Load		KHN (GPa) ^a		
		(g)	(N)	Average	Max.	Min.
J. Brynstad	Sintered rod	15	0.147	2.21	2.34	1.98
		25	0.245	2.78	3.58	2.32
		50	0.491	3.78	4.37	3.19
R. Poeppel	Sintered disk	15	0.147	2.33	2.61	1.85
		25	0.245	3.05	3.65	2.68
L. Boatner	Crystal No. 1	15	0.147	3.54	4.10	2.98
		25	0.245	3.43	3.51	3.35
	Crystal No. 2	15	0.147	3.55	3.80	3.30
		25	0.245	4.53	4.75	4.15

^aAverage of two to six clear impressions for each value reported.

3.2. NANOINDENTATION EXPERIMENTS

Additional hardness experiments using a very low-load, shallow-penetration mechanical properties microprobe (Nanoindenter™) were performed. This instrument measures the load-displacement behavior of a triangular pyramidal indenter and allows computation of both indentation hardness and elastic modulus as a continuous function of load and penetration depth. Figure 4 shows a schematic diagram of the Nanoindenter, and Fig. 5 shows a typical load-displacement curve for a specimen of 1-2-3 in terms of the raw voltage outputs to the computer. The elastic modulus is computed from the slope of the off-loading portion of the load vs displacement curve. The approach rate, loading rate, dwell at maximum depth, hold at partially released load (to check for drift), and thermal drift corrections are all selected prior to the experiment. Figure 6 shows a series of tiny impressions on a polycrystalline 1-2-3 specimen indicating a preset pattern of nanoindentations.

Table 3 gives the nanoindentation hardness and elastic modulus for two types of 1-2-3 specimens: the thin single crystals grown at ORNL and the polycrystalline material provided by ANL. For the ANL specimen, the indentation array covered several crystal grains, but for the single

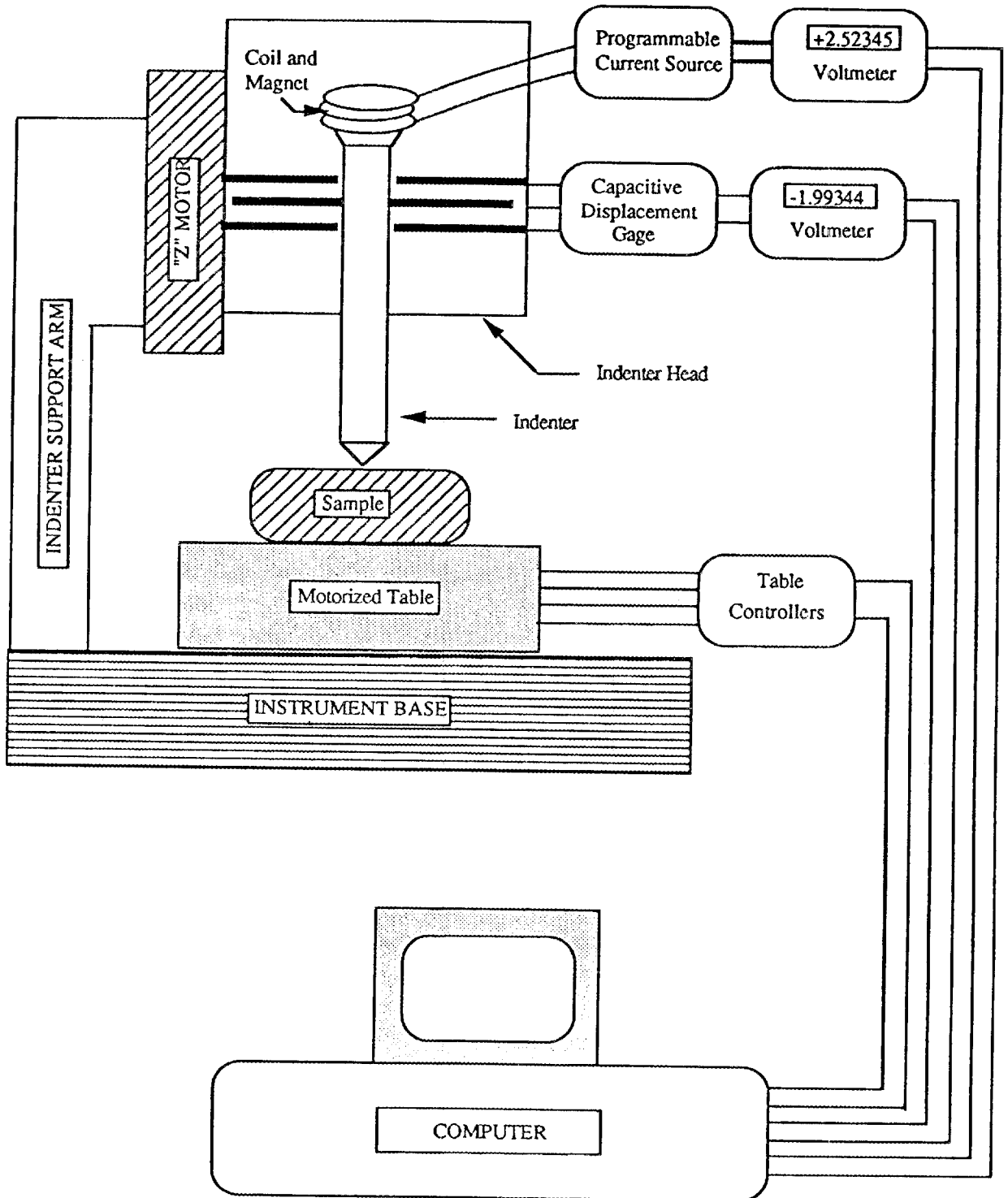


Fig. 4. Schematic diagram of the Nanoindenter™.

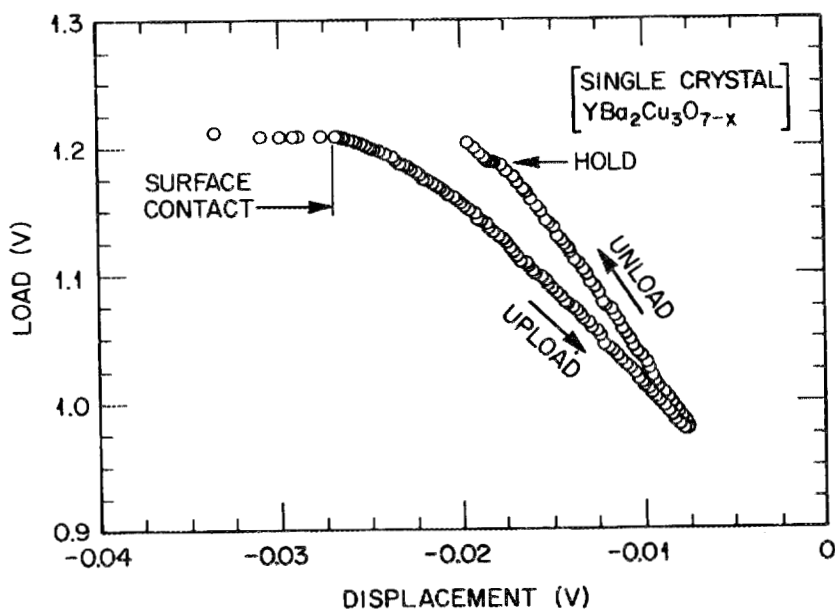


Fig. 5. Typical raw data for sensor voltages used to construct a load-displacement curve for an individual indentation experiment on 1-2-3.

crystal, all indents were approximately parallel to the c -axis of the crystal [i.e., normal to the (001) plane].

As might be expected, the scatter in the data for the polycrystalline specimen was greater than that for the single crystal specimen. Since the applied load and indenter geometry differed between the Knoop microindentation experiments and the Nanoindenter measurements, the hardness numbers should not be directly compared. Furthermore, the Nanoindenter values for hardness contain a correction for elastic recovery of the indentations, and the Knoop microindentation hardness numbers are obtained from the long diagonal lengths of elastically recovered impressions.

The values of the current indentation-derived modulus of elasticity deviate substantially from the 235 ± 20 GPa reported by Block et al.,¹⁷ who derived their value from X-ray diffraction data and from the bulk modulus obtained from the dependence of atomic volume on applied pressure. They also differed from the 226 GPa reported by Chang et al.,¹² who used a 6.35-mm-diam (1/4-in.) tungsten carbide sphere for their indenter. The

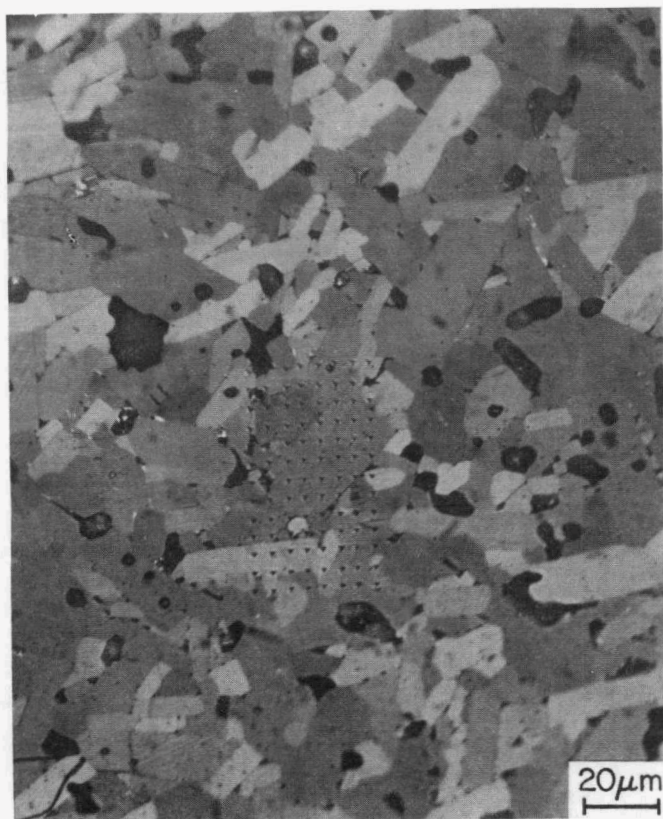


Fig. 6. Pattern of triangular indentations extending across several grain boundaries in a Brynstad specimen which was 93% dense.

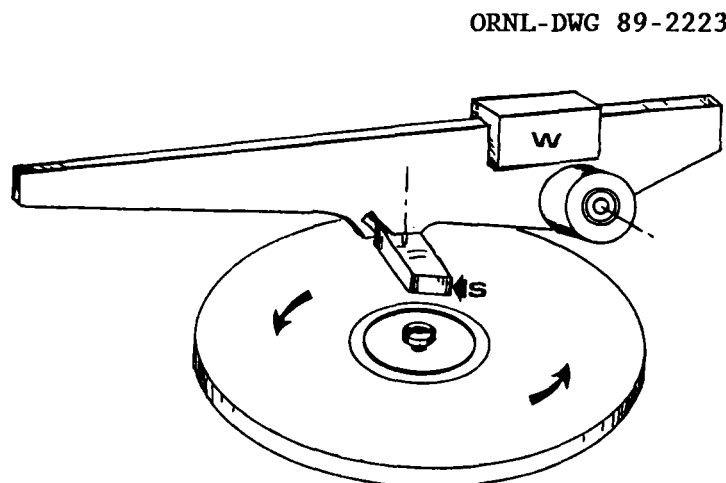
Table 3. Nanoindentation properties of $\text{YBa}_2\text{Cu}_3\text{O}_{7-x}$
(25 values per material recorded at a penetration depth of 200 nm)

Material type	Hardness number (GPa)	Young's modulus (GPa)
Single crystal	3.93 ± 0.45	78.56 ± 4.41
Polycrystalline	3.62 ± 0.56	81.72 ± 9.64

current indentation-derived Young's modulus values agree better with the values of Ledbetter et al.,⁹ who reported a density-corrected elastic modulus of 90.8 to 101.8 GPa, and with Blendell et al.,¹⁸ who reported a porosity-corrected, ultrasonically measured Young's modulus of 139 GPa. The wide range of values of Young's modulus reported in the literature for 1-2-3 results from the application of a range of techniques to characterize materials which undoubtedly had different microstructures and densities. More work using larger single crystals with known crystallographic orientations is needed before the modulus can be determined with a high level of confidence in the accuracy of the results.

3.3. SCRATCH HARDNESS TESTING

Scratch tests were performed on a portable commercial scratch testing machine (Teledyne Taber Shear/Scratch Tester). This device consists of a rotating flat table, on which the specimen is affixed, and a balance beam-mounted diamond stylus with a measured hemispherical tip radius of $74.1 \mu\text{m}$ (Fig. 7). Tests were performed on a specimen of the Brynestad rod material



W = WEIGHT FOR APPLYING NORMAL FORCE
S = SPECIMEN

Fig. 7. Diagram of the scratch tester used in this study.

(1.5 cm long \times 0.4 cm in diameter) which had been metallographically polished to expose a rectangular longitudinal section. Scratches were made in air at 0.25, 0.49, 0.73, and 0.98 N load at a sliding velocity of 0.2 cm/s. Scratch widths were difficult to measure accurately by optical microscopy at 500X due to irregularities in the damage at the scratch edges; therefore, an uncertainty of about $\pm 15\%$ is estimated for these data.

Bearing in mind the uncertainties in scratch width measurement, average scratch widths were linearly related to the stylus load as follows:

$$W = 0.228L + 3.5 , \quad (1)$$

where L is stylus load in grams and W is nominal scratch width in micrometers. The correlation coefficient (R) for the data fit to Eq. (1) was 0.9991, a somewhat surprising correlation in view of the uncertainties in the width measurements.

The scratch hardness (based on scratch width) of the superconductor materials is compared with earlier data for several metals¹⁷ in Fig. 8. The scratch hardness numbers (SHN) were obtained from

$$\text{SHN} = (L/A) , \quad (2)$$

where L is load and A is the load-supporting area during scratching. The load-supporting area is assumed to be the leading half of the surface of a spherical cap of radius (r) equal to 74.1 μm (the measured stylus tip radius) and base w , the scratch width in micrometers. Area is calculated from

$$A = \pi r^2 [1 - \cos X] , \quad (3)$$

where $X = \sin^{-1} (w/2r)$. The superconductor displayed a drop in SHN with increasing stylus load. This, in contrast to the more ductile metals, indicates a decreasing resistance to scratching as load increases. The increase in cracking at the higher load is shown in Fig. 9.

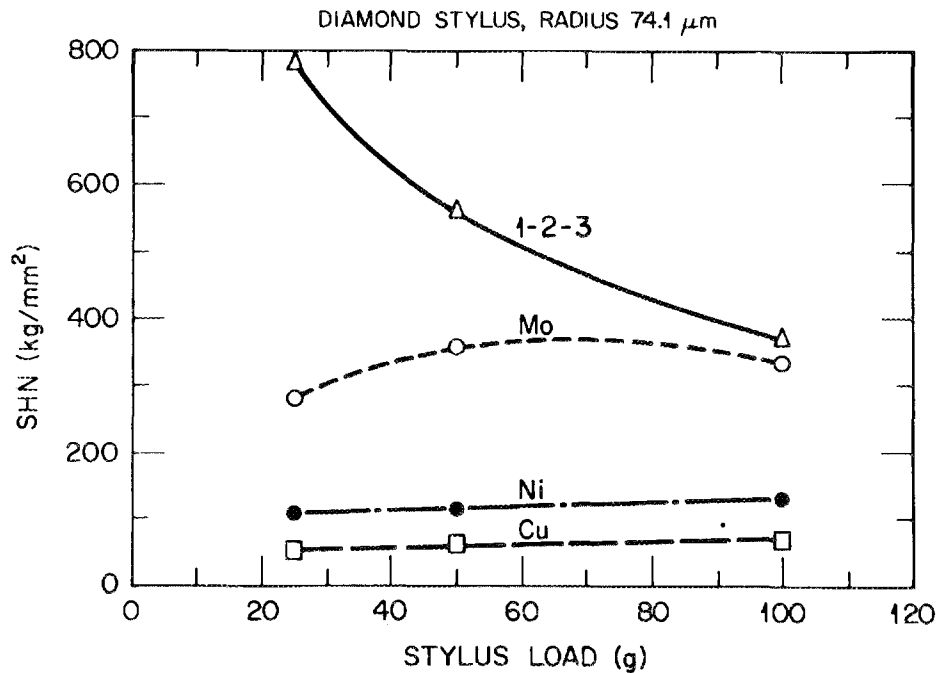


Fig. 8. Comparison of scratch testing data for 1-2-3 and several pure metals showing a decline in scratch hardness numbers (SHN) with increasing load.

In summary, the scratch resistance of the 1-2-3 material can be relatively high only if loads can be kept below those which produce substantial intergranular and transgranular cracking. This point is consistent with the well-established concept of a critical load for fracture in brittle materials. Unfortunately, the surface appearance of the 1-2-3 polycrystalline specimens in the present investigation was such that it was not possible to unambiguously distinguish the critical scratching load below which no fracture occurred. In the next section, the abrasion of 1-2-3 by multiple asperities (abrasive paper) is discussed further.

3.4. ABRASION EXPERIMENT

To study the nature of surface damage due to two-body abrasion of 1-2-3, a 2.0-cm-diam disk of the ANL material was slid against silicon

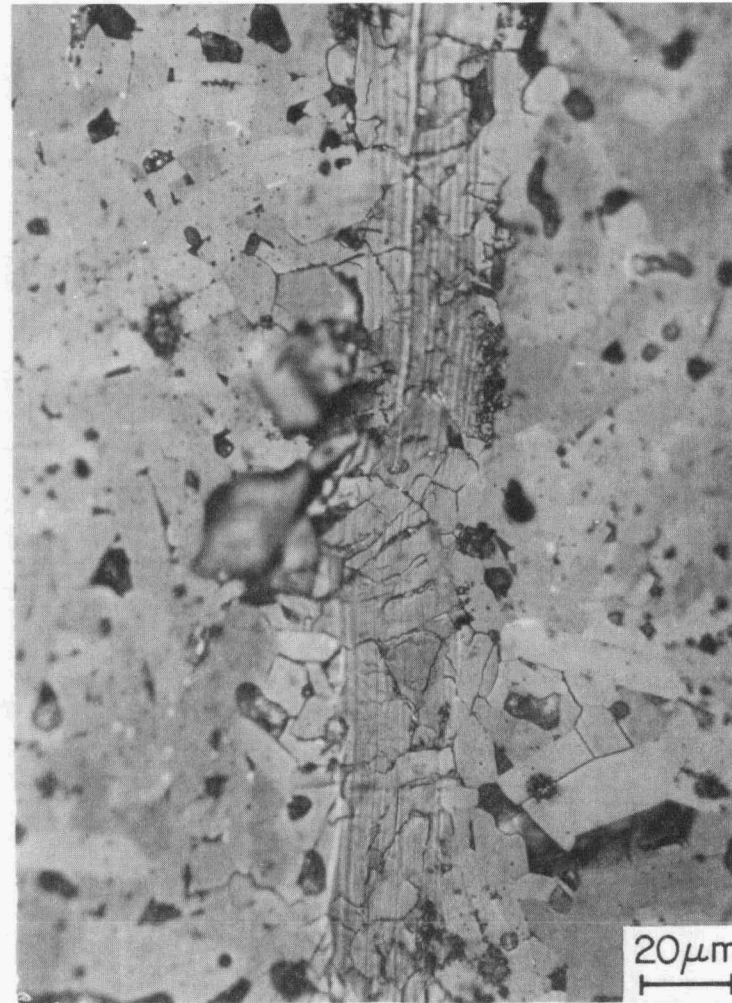
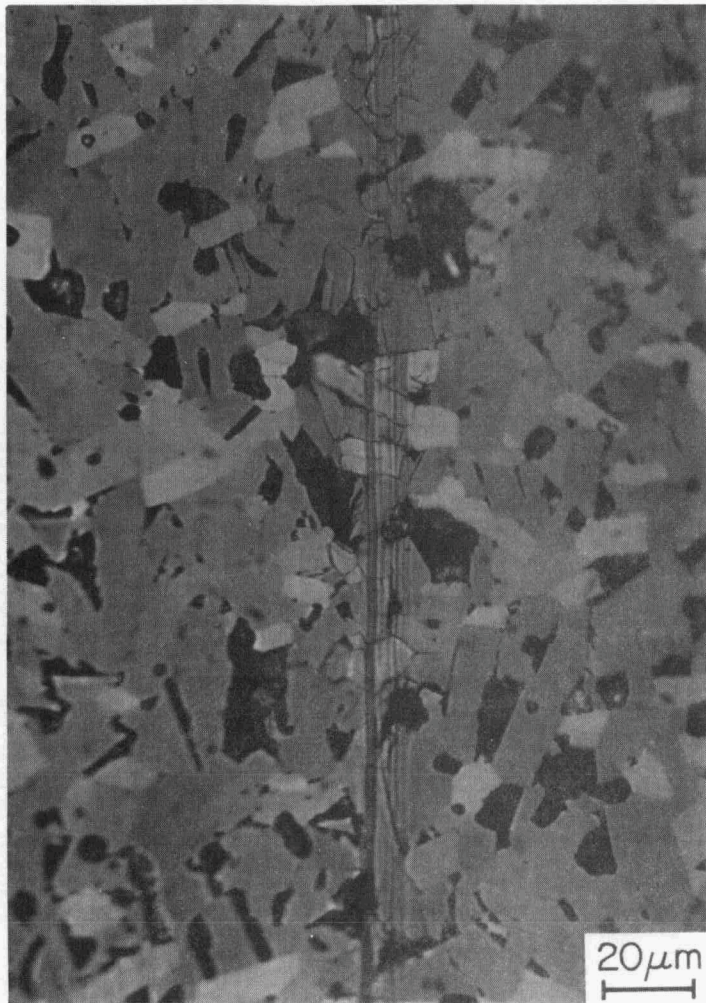


Fig. 9. Scratch damage to the rod material at 25-g (left) and 100-g (right) stylus loads (original mag. 500X).

carbide abrasive paper and examined in the scanning electron microscope. The conditions of the abrasion experiment were as follows:

- normal force: 4.91 and 9.81 N (dead-weighted);
- velocity of sliding: 5.0 cm/s;
- specimen surface preparation: 600-grit finish by dry grinding;
- stroke length: 20.0 cm (unidirectional, not reversed sliding);
- number of strokes: 25 (offset after each pass to contact new abrasive);
- abrasive: 180-grit (70 μm particles) SiC paper;
- temperature: 22°C (295 K); and
- relative humidity: 77% (wet bulb-dry bulb method).

The mass loss during the 4.91-N experiment was 0.0265 g and during the 9.81-N experiment was 0.0509 g. A theoretical density of 6.357 g/cm³ (ref. 20) gave abrasive wear coefficients of 0.170 mm³/N-m and 0.327 mm³/N-m, respectively. The ratio of wear coefficients for the two normal loads was 1.92 compared with a normal load ratio of 2. Therefore, wear rate was approximately in direct linear proportion to test load. There appeared to be no significant damage to the silicon carbide paper after the experiment, and a jet of air removed almost all visible evidence that the experiment had been performed. This is not particularly surprising considering that the hardness of the two materials (1-2-3 and SiC) varied by a factor of 4.5.

Optical and scanning electron microscopy revealed severe surface damage on the 1-2-3 specimen. Many types of microfracture were observed, including ductile tearing in grooves cut by the abrading particles, and transgranular and intergranular fracture. Figures 10 and 11 show typical damage structures on the abraded specimen surface. The fine, angular debris is typical of brittle materials undergoing abrasion. In the abrasion of more ductile materials, thin, feathery chips similar to those observed in machining would be produced. Beneath the tips of the asperities which groove the surface, the hydrostatic stress promotes enhanced ductility and, consequently, more ductile features can be observed; but adjacent to the grooves, brittle fracture is extensive. The abrasion resistance of 1-2-3 under the conditions of these experiments was not good.



Fig. 10. Area of an abraded specimen showing long grooves (horizontal) characteristic of abrasion (scanning electron micrograph).

3.5. RECIPROCATING SLIDING FRICTION AND WEAR TESTS

The tribometer used in this work used a back-and-forth sliding arrangement (sphere-on-flat geometry) with a stroke length of about 0.5 cm. The fixturing and friction-measuring arrangement is shown in Fig. 12. In these experiments, gold (a primary constituent metal used for many types of



Fig. 11. Higher magnification scanning electron micrograph of a single groove showing ductile tearing in the groove and brittle fracture beside it.

electrical connectors) and 1-2-3 were used as counterface materials. The gold sliders, nominally 0.3 cm in diameter, were created by melting a bead on the end of gold wire. The 1-2-3 sliders were created from the Brynstad material in two ways: (1) by wafer-sawing 2- to 3-mm-thick disks from the end of a rod and mounting them such that the cylindrical surface of the disk was tangent to the flat surface and in line with the back-and-forth

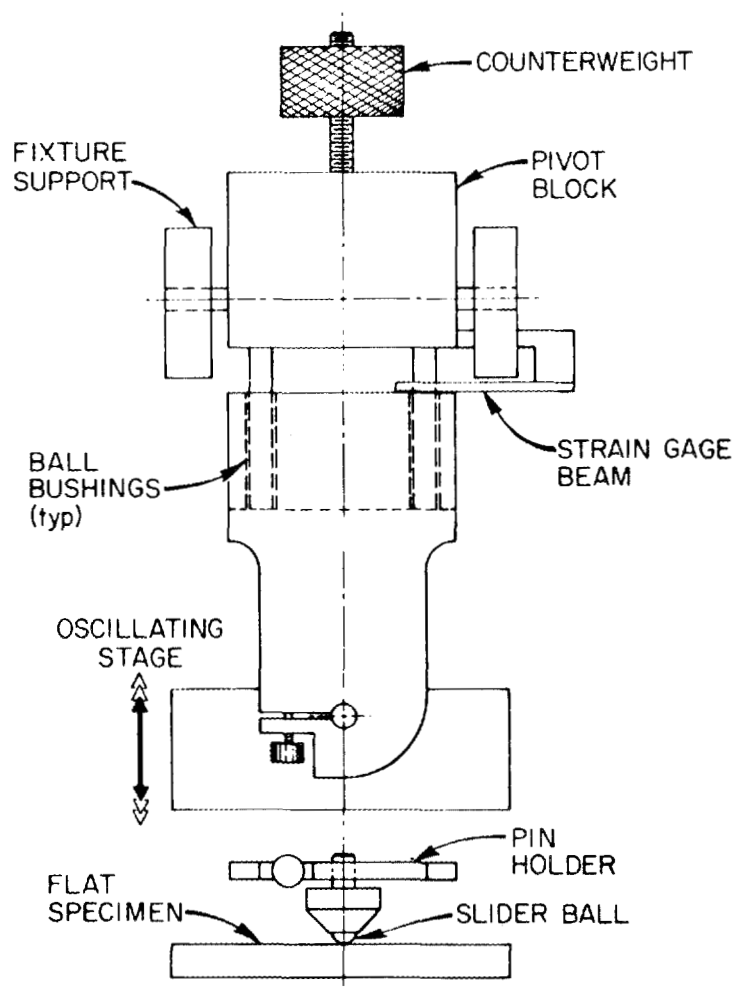


Fig. 12. Diagram of the reciprocating friction testing apparatus and the slider holder arrangement.

sliding direction, and (2) by polishing hemispherical tips of 4.7-mm radius on rod ends. The latter method proved more effective in obtaining reproducible friction results. The configuration of the sliders are shown in Fig. 13.

Tests were conducted in air using loads of 0.981 and 1.96 N. The frequency of oscillation was about one full cycle (i.e., a complete stroke in each direction) in 6 s. Friction force was obtained from a strain-gauged force-sensing beam on the pin fixture by a digital voltmeter

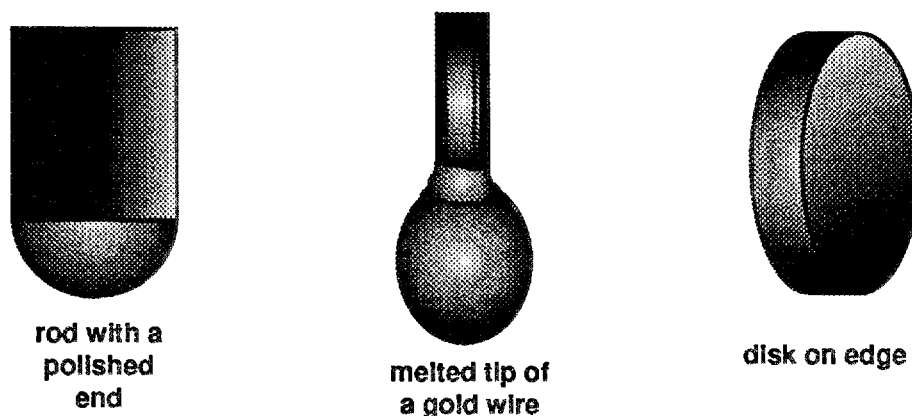


Fig. 13. Slider configurations for sliding friction and wear tests.

interfaced to a desktop computer at a sampling rate of one reading per 0.01 s. Test lengths varied between 10 and 1000 cycles in these experiments.

Friction coefficient data for gold sliding unlubricated on the Poeppel and Brynstad samples are given in Figs. 14(a) and 15. At the beginnings of all but one run, friction coefficients were relatively low (0.12 to 0.35); however, they rose quickly (within the first 10 cycles) to high values (over 0.9). Then they declined gradually until the run ended. One of the runs with a gold slider, depicted in Fig. 15, began higher than the others ($\mu = 0.92$). There were no obvious clues to this behavior based on posttest surface examination, and the reason for the anomaly remains unclear.

In the early experiments which compared the 93% dense material with the 98% dense material, the friction coefficients of the more porous samples rose more quickly than those for the denser material. Examination of the wear tracks showed gold trapped in surface pores (Fig. 16) after only 10 cycles of sliding; and after longer sliding times, a dark gray transfer film was observed not only on the surface of the track, but also on the ball tips (Fig. 17). Development of this film is believed responsible for the climb in friction. Sharp edges of exposed pores of the

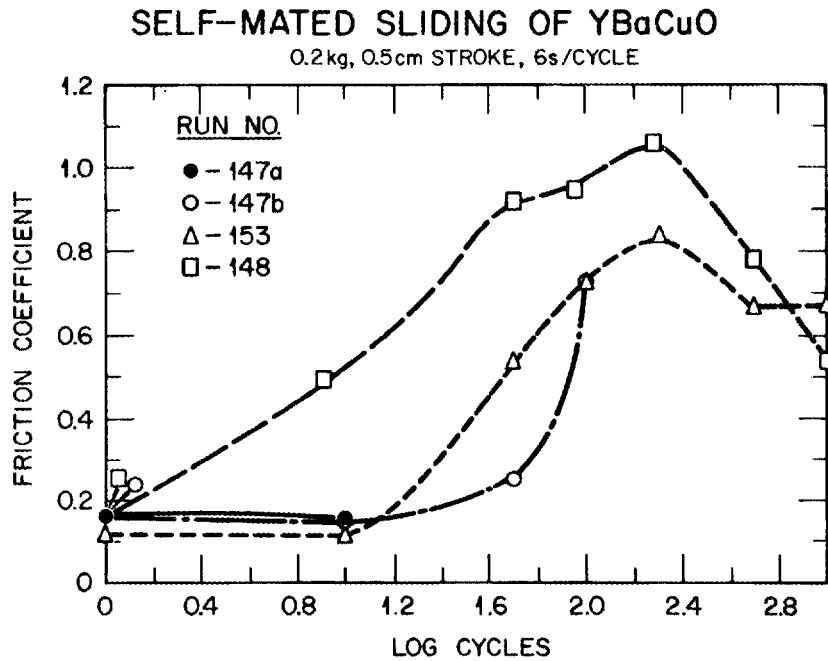
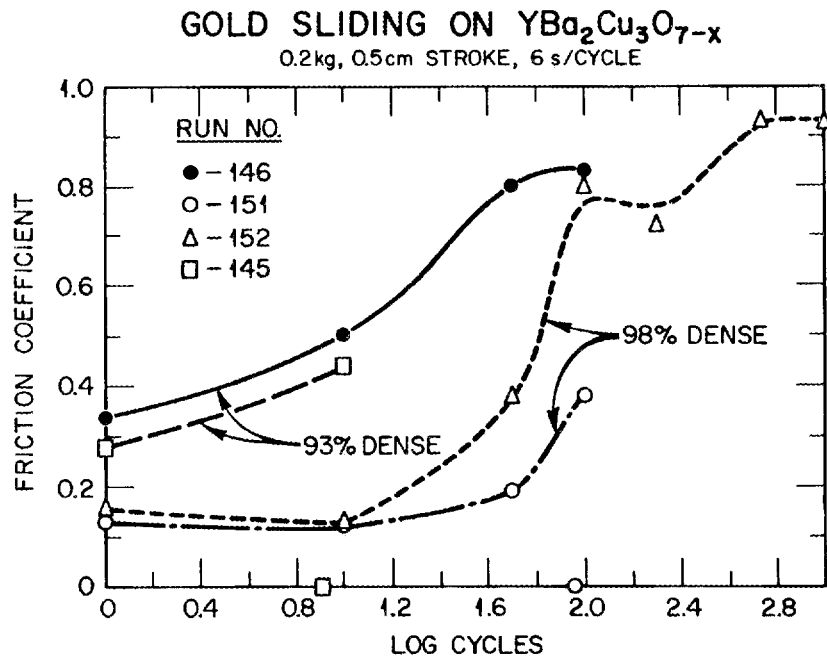


Fig. 14. Friction coefficient vs log sliding cycles for tests at 1.96 N load.

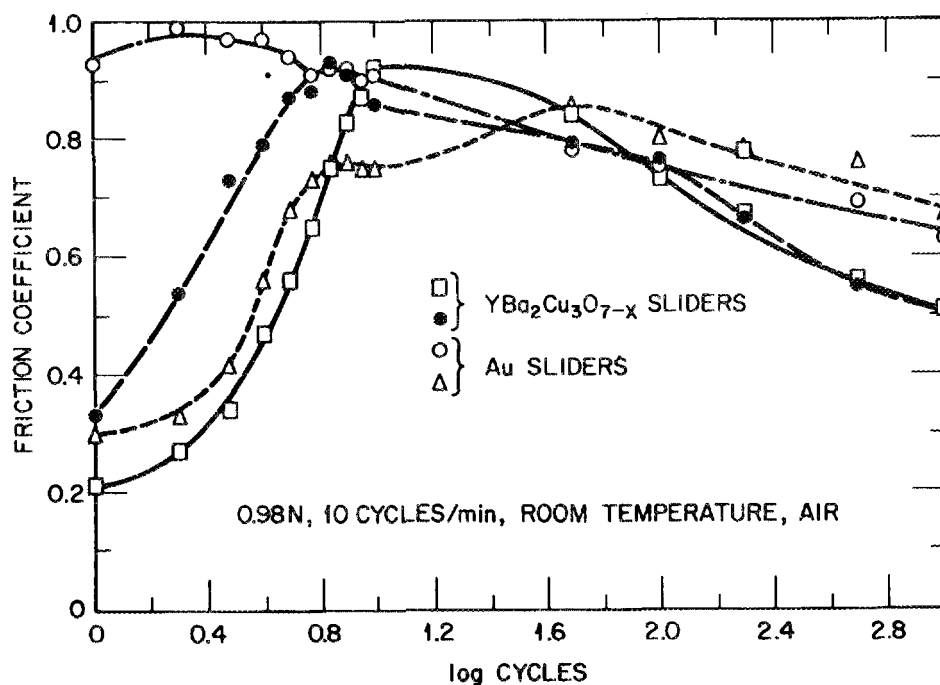


Fig. 15. Friction coefficient vs log sliding cycles for tests at 0.98 N load.

less-dense material may have shaved gold from the slider and led to an earlier transition to high friction. On the denser material, the transfer film formed more gradually, but once formed, produced quite high friction coefficients. While there was a dark deposit on the gold slider tip, there was no direct evidence by optical microscopy that 1-2-3 debris embedment in the gold was leading to track abrasion.

One cause for the eventual fall in friction observed in all 1000-cycle runs may have been the progressive wear of the tracks, creating open areas which could trap wear debris which might otherwise contribute to higher sliding friction forces. The gold track displayed transfer films, and the 1-2-3 track showed the open areas, which are one possible reason for the decline in the friction coefficient at the end of the longer tests. The use of modulated surfaces for friction control by promoting debris trapping is discussed by Suh.²¹ This concept has been further exploited by a patent by Suh et al.²²

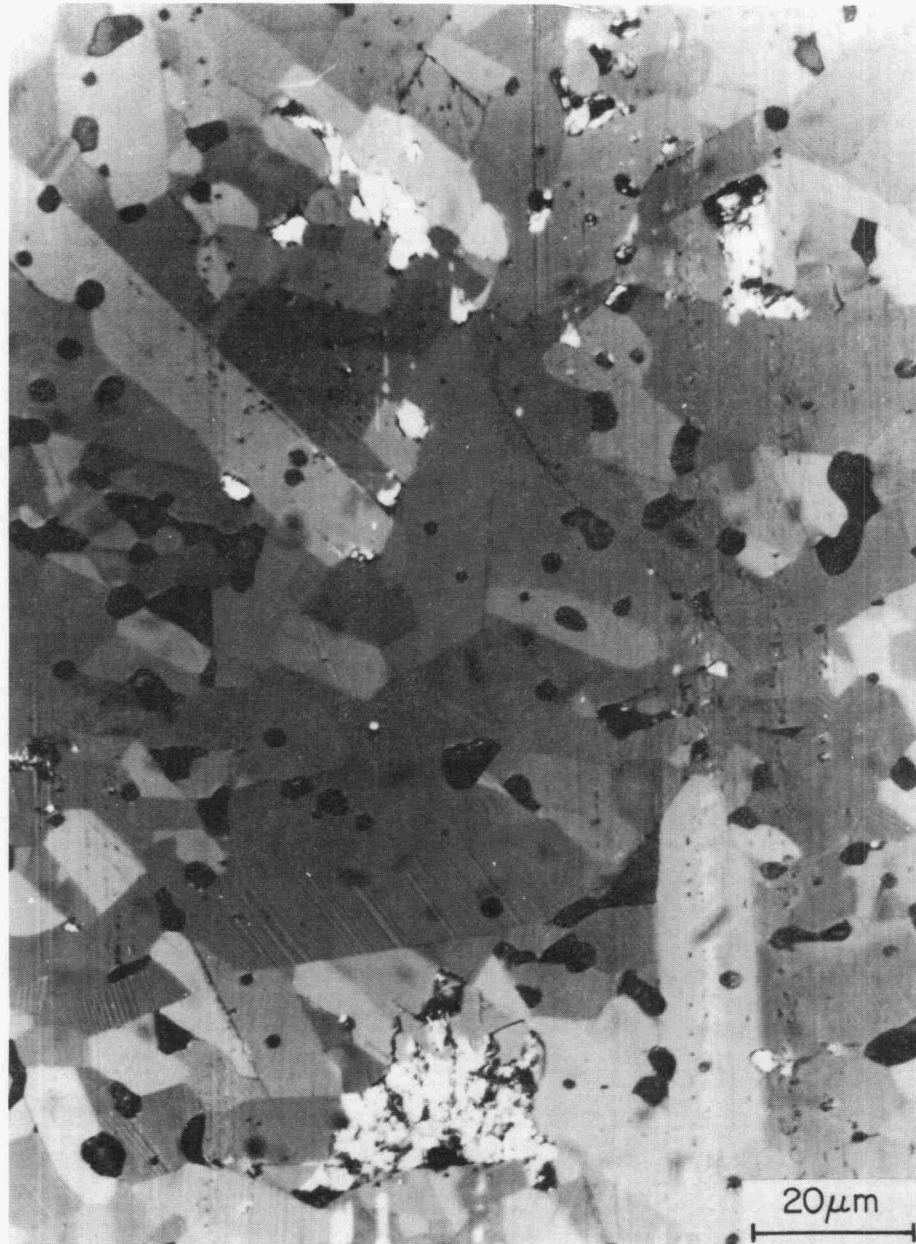


Fig. 16. Gold-filled pores on the sliding surface of the Brynstad material (original mag. 500X).

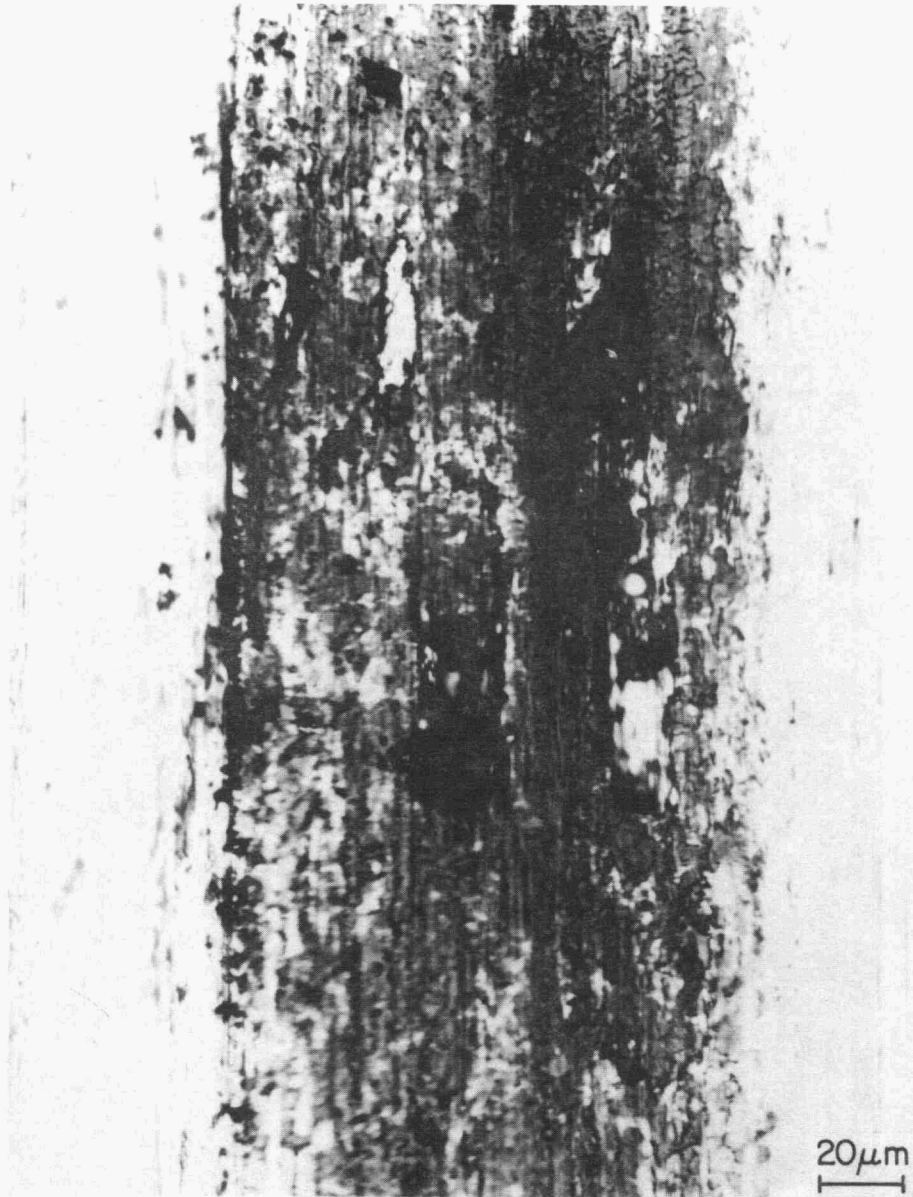


Fig. 17. Dark transfer film, possibly friction polymer, on the tip of the gold slider (original mag. 500X).

Another possible reason for the decrease in friction with increasing cycle number concerns the presence of fine, needle-like debris particles which were frequently observed to lay across the track, perpendicular to the sliding direction. These cylindrical needles were typically under $0.5 \mu\text{m}$ in diameter and as long as $6 \mu\text{m}$. Many such needles can be seen in Fig. 18 where they have been captured by a pocket in the wear surface. The diameter of the needles was similar to the width of fine twins, which were visible in polarized light. From these observations, it is proposed that the early stages of wear can involve the microfracture of grains along twin boundaries. The needle-like debris particles then act as tiny rollers to reduce the friction along the sliding path.

One final observation on the 1-2-3 materials we examined regards the alleged moisture sensitivity of the compound. In our experience there was no obvious microstructural evidence of degradation due to exposure to lab air during testing or examination. Specimens polished several months before reexamination displayed no evidence of grain-boundary decohesion or surface reactions.

3.6. UNIDIRECTIONAL SLIDING FRICTION AND WEAR TESTS

Unidirectional sliding friction and wear tests were performed on as-received (fine-ground) specimens from Lambertville Ceramics, Inc. (HiTc Superconco). The microstructure of this material is shown in Fig. 19. The upper fixture which held the hemispherically tipped 1-2-3 slider (Brynestad material) was of the same design as that used for the reciprocating tests, but the lower specimen rotated in one direction instead of moving back and forth (Fig. 20). Test conditions were as follows:

- load: 1.0 N (similar to the 0.98 N used in the reciprocating tests),
- velocity: 0.1 m/s,
- test duration: 100 m sliding distance, and
- environment: room temperature air.

Note that original plans called for a test length of 1000 m, but the wear rate was so high that 100-m tests were conducted. Wear rates were obtained from stylus traces of the disk track profile.



Fig. 18. Needle-like debris caught in a pore on the sliding surface from a self-mated test.

Table 4 lists the results of the unidirectional sliding wear experiments. Both friction and wear were quite high, further supporting the reciprocating wear data which portrayed 1-2-3 as a poor tribomaterial. Unlubricated ceramics in mild wear regimes can have sliding friction coefficients between about 0.2 and 0.5, but usually do not reach the steady-state values reported in Table 4 unless they are undergoing severe

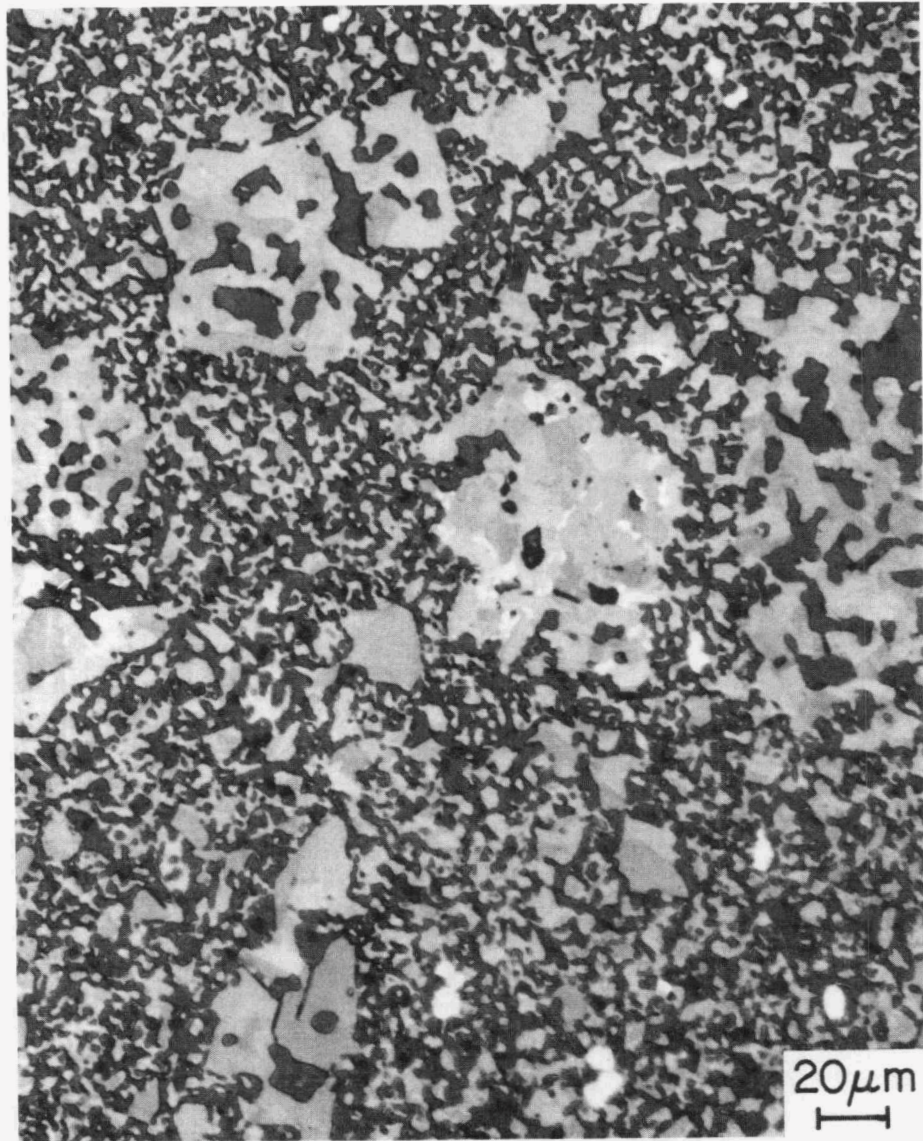


Fig. 19. Microstructure of commercially prepared 1-2-3. The quality of this polyphase material was inferior to that of the Argonne materials in that the disks were often found to contain hairline cracks running across them. They had to be handled carefully during polishing and testing to make sure they did not fracture.

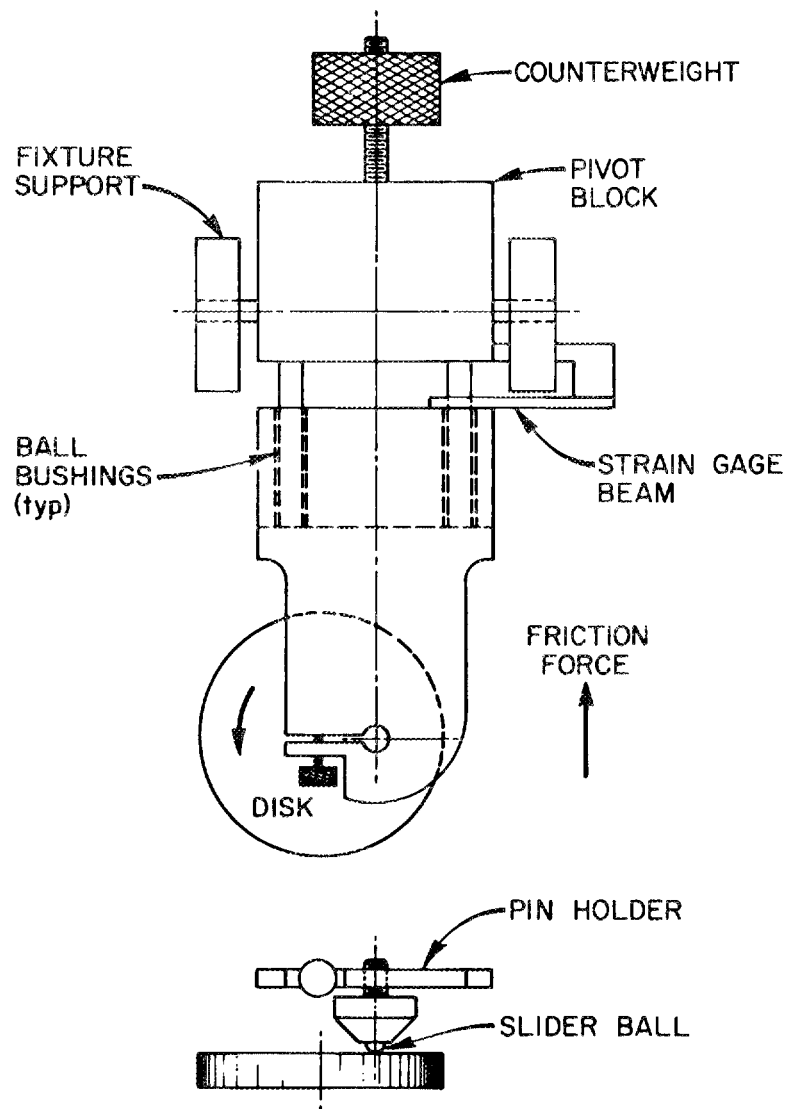


Fig. 20. Schematic diagram of the pin-on-disk tribometer used for unidirectional sliding experiments. The friction force sensing arrangement was similar to that in Fig. 12.

wear which results in the pronounced surface roughening and the accumulation of debris. Indeed, the very high wear rates in Table 4 substantiate this point. Ceramics undergoing mild wear generally have wear rates in the 10^{-7} to 10^{-10} $\text{mm}^3/\text{N}\cdot\text{m}$ range.

Table 4. Unidirectional sliding friction and wear of $\text{YBa}_2\text{Cu}_3\text{O}_{7-x}$

Run	Friction coefficient			Wear rate ($\text{mm}^3/\text{N}\cdot\text{m}$)
	Initial	Maximum observed	Steady state	
1	0.29	1.03	0.75	7.31×10^{-2}
2	0.33	0.85	0.70	7.35×10^{-2}

X-ray diffraction was performed at the ORNL High Temperature Materials Laboratory Materials Characterization User Center on the debris particles to see whether any had transformed from the superconducting orthorhombic phase to a nonsuperconducting phase, but the debris had lattice parameters expected for the orthorhombic phase. These lattice parameters were $a = 0.38240$ nm, $b = 0.38864$ nm, and $c = 0.16694$ nm. These values compared favorably with previous X-ray powder data for 1-2-3 reported by Wong-Ng et al.;²³ namely, $a = 0.38214$ nm, $b = 0.38877$ nm, and $c = 1.1693$ nm. A small amount of BaCuO_2 was barely detectable in the debris powder. This may have come from residual grain boundary material; however, the source of the BaCuO_2 was not identified in this investigation. X-ray results indicated that there was no apparent shear deformation-induced crystallographic transformation of 1-2-3 which occurred as a result of sliding contact.

Photomicrographs of the granular debris on the wear track are given in Fig. 21. None of the needle-like particles observed on the reciprocating wear tracks were observed on the unidirectional sliding tracks. Instead, the debris was more blocky. Figure 22 shows that the debris layer was compressed and plastically sheared at some locations on the wear track. There was so much debris adhering to the wear track that none of the worn surface was visible through the debris layer. These observations indicate that third bodies (i.e., debris particles) play a major role in the unlubricated sliding wear of 1-2-3.

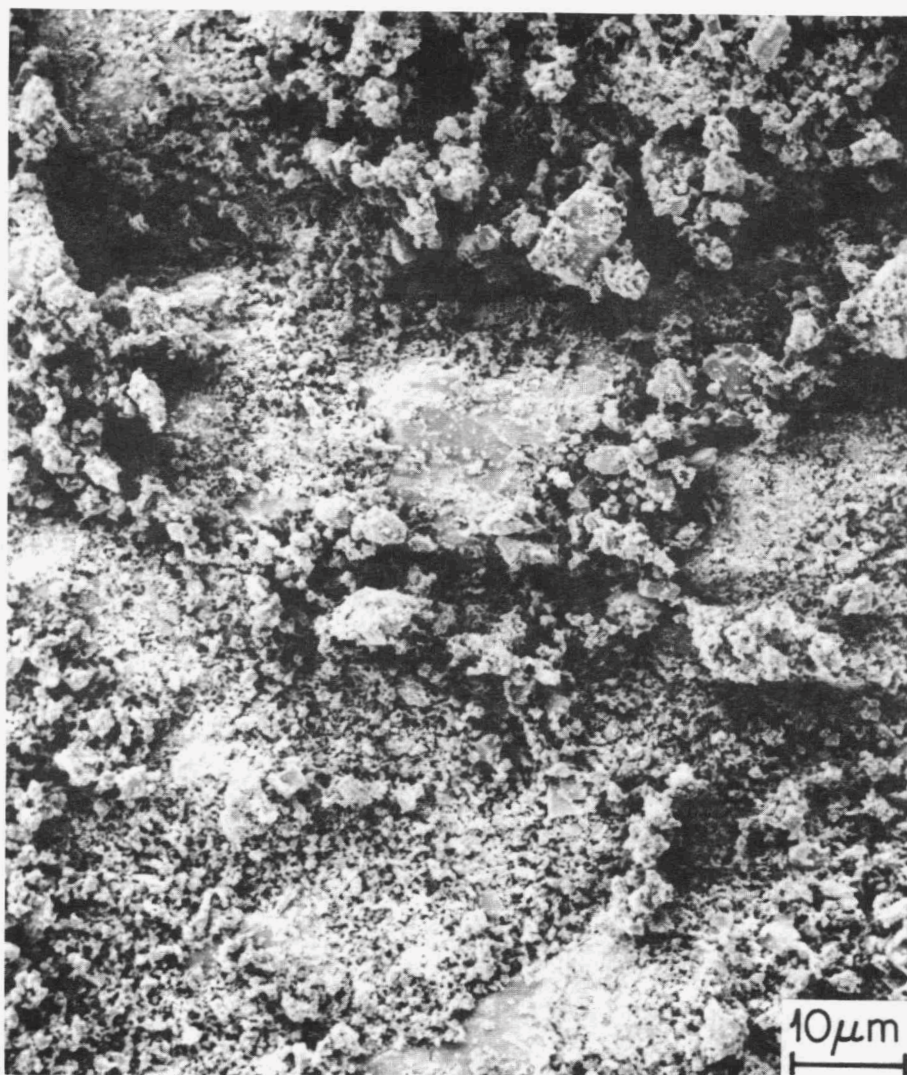


Fig. 21. Scanning electron micrograph of pulverized debris covering the wear track. Sizes ranged from less than $1\ \mu\text{m}$ to several micrometers.

4. SUMMARY AND CONCLUSIONS

The indentation hardness (two types), elastic modulus, scratch hardness, two-body abrasion, friction, and sliding wear of $\text{YBa}_2\text{Cu}_3\text{O}_{7-x}$ obtained from five sources were studied with the following results:

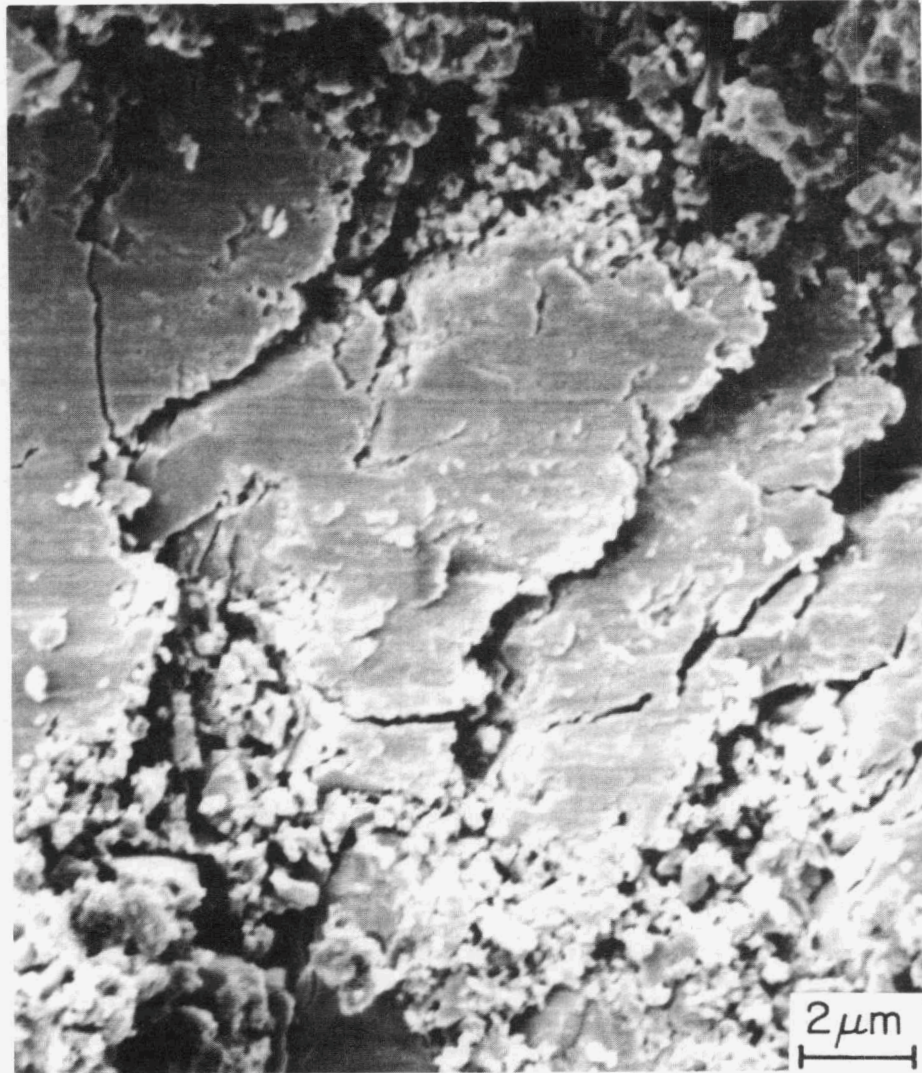


Fig. 22. Scanning electron micrograph showing that once debris compacts formed, they could shear plastically.

1. The $\text{YBa}_2\text{Cu}_3\text{O}_{7-x}$ we tested was brittle and sensitive to scratching and two-body abrasion.
2. The indentation hardness of the material is relatively low for a ceramic (between that for hardened brass and bearing steel).

3. The unlubricated sliding friction coefficients against itself or gold generally start below 0.4, build up to above 0.9 after about 10 cycles, then gradually decline as wear progresses.

4. Wear occurs by fracture on two scales, one on the order of the twin spacing and the other on a transgranular and intergranular scale.

5. Unless the material can be contained within a composite of better durability, there is little optimism for using this material in abrasive or sliding contact situations.

Applications such as electrical contacts are possible only when load is low and mechanical movement is carefully controlled. Applications such as motor brushes must await further advances in material processing or lubrication technology as well as a better understanding of the effects of sliding-induced damage on superconductivity.

ACKNOWLEDGMENTS

The authors wish to acknowledge J. Brynestad and L. A. Boatner, Oak Ridge National Laboratory; R. B. Poeppel and K. C. Goretta, Argonne National Laboratory; and D. Varacalle, Jr., Idaho National Engineering Laboratory, for supplying specimen materials. X-ray analysis was conducted by O. B. Cavin. The advice of A. C. Schaffhauser, Director of the ORNL Superconductivity Pilot Center, is appreciated.

REFERENCES

1. K. A. Müller and J. G. Bednorz, "The Discovery of a Class of High Temperature Superconductors," *Science* **237**, 1133-39 (1987).
2. M. M. Waldrop, "The 1987 Nobel Prize for Physics," *Science* **238**, 481-82 (1987).
3. H. K. Bowen, "Ceramic Superconductors," *Ceram. Bull.* **66**, 1191-96 (1987).
4. G. Fisher and M. Schober, "Ceramic Superconductor Research Pace Quickens," *Ceram. Bull.* **66**, 1087-94 (1987).
5. A. L. Robinson, "Commercialization of Superconductors Spurs International Competition," *MRS Bull.*, 48 (June/August 1987).

6. W. Lepkowski, "Superconductivity Drive Sparks New Policy Debates," *Chem. Eng. News*, 10-14 (September 7, 1987).
7. J. Douglas, "Pursuing the Promise of Superconductivity," *Electr. Power Res. J.*, 5-15 (September 1987).
8. L. C. Bourne et al., "Elasticity Studies of $\text{La}_{2-x}\text{Sr}_2\text{CuO}_4$," *Phys. Rev. B* 35(16), 8785-87 (1987).
9. H. M. Ledbetter et al., "Elastic Constants and Debye Temperatures of Polycrystalline $\text{Y}_1\text{Ba}_2\text{Cu}_3\text{O}_{7-x}$," *J. Mater. Res.* 2(6), 786-89 (1987).
10. H. M. Ledbetter et al., "Shear Modulus Change Below T_c in $\text{YBa}_2\text{Cu}_3\text{O}_{7-x}$," *J. Mater. Res.* 2(6), 790-92 (1987).
11. R. F. Cook, T. R. Dinger, and D. R. Clarke, "Fracture Toughness of Measurements of $\text{YBa}_2\text{Cu}_3\text{O}_x$ Single Crystals," *Appl. Phys. Lett.* 51, 454 (1987).
12. G. C. S. Chang et al., "Young's Modulus Measurement of Polycrystalline $\text{YBa}_2\text{Cu}_3\text{O}_{7-d}$ Superconductor," *Proc. Am. Ceram. Soc.*, in press.
13. D. Erskin et al., "Pressure Dependence of Superconducting Transition Temperature in $\text{La}_{1.85}\text{Sr}_{0.15}\text{CuO}_4$ to 8 GPa," *J. Mater. Res.* 2(6), 783-85 (1987).
14. S. I. Park et al., "Effect of Uniaxial Strain on the Superconducting Transition Temperature in Thin $\text{YBa}_2\text{Cu}_3\text{O}_7$ Film," *Proc. Mater. Res. Soc., Fall Meeting* (1987).
15. R. Pool, "Superconductivity Result Unconfirmed," *Science* 241, 1038 (1988).
16. J. D. Livingston, A. R. Gaddipati, and R. H. Arendt, "Metallographic Studies of Sintered $\text{Y}_1\text{Ba}_2\text{Cu}_3\text{O}_{7-x}$," *Proc. Mater. Res. Soc., Fall Meeting* (1987), p. 931.
17. S. Block et al., "The Bulk Modulus and Young's Modulus of the Superconductor $\text{Ba}_2\text{Cu}_3\text{YO}_7$," *Adv. Ceram. Mater.*, (special supplement issue) 2(3B), 601-05 (1987).
18. J. E. Blendell et al., "Processing-Property Relations for $\text{Ba}_2\text{YCu}_3\text{O}_{7-x}$ High T_c Superconductors," *Adv. Ceram. Mater.*, (special supplement issue) 2(3B), 512-29 (1987).

19. P. J. Blau, "Relationship Between Scratch and Knoop Microindentation Hardness and Implications for Abrasion of Metals," *Microstruct. Sci.* 12, 293 (1985).
20. R. J. Cava et al., "Bulk Superconductivity at 91K in a Single Phase Oxygen Deficient Perovskite $\text{D}_{a_2}\text{YCu}_3\text{O}_{9-\delta}$," *Phys. Rev. Lett.* 58, 1676 (1987).
21. N. P. Suh, *Tribophysics*, Prentice-Hall, Englewood Cliffs, N.J., 1986.
22. N. P. Suh, N. Saka, and M. J. Liou, "Electrical Contacts," U.S. Patent No. 4,687,274, Aug. 18, 1987.
23. W. Wong-Ng et al., "X-Ray Powder Characterization of $\text{Ba}_2\text{YCu}_3\text{O}_{7-x}$," *Adv. Ceram. Mater.*, (special supplement issue) 2(3B), 565 (1987).

INTERNAL DISTRIBUTION

- | | | | |
|--------|-------------------------------|--------|----------------------------------|
| 1-2. | Central Research Library | 74-78. | J. R. Keiser |
| 3. | Document Reference Section | 79. | H. E. Kim |
| 4-5. | Laboratory Records Department | 80. | W. S. Koncinski, Jr. |
| 6. | Laboratory Records, ORNL RC | 81. | D. M. Kroeger |
| 7. | ORNL Patent Section | 82. | E. H. Lee |
| 8-10. | M&C Records Office | 83. | A. C. Schaffhauser |
| 11. | R. L. Beatty | 84. | V. K. Sikka |
| 12. | T. M. Besmann | 85. | G. M. Slaughter |
| 13-62. | P. J. Blau | 86. | J. O. Stiegler |
| 63. | R. A. Bradley | 87-91. | D. F. Wilson |
| 64. | R. S. Carlsmith | 92. | A. D. Brailsford (Consultant) |
| 65. | G. M. Caton | 93. | H. D. Brody (Consultant) |
| 66. | D. F. Craig | 94. | F. F. Lange (Consultant) |
| 67-71. | C. E. DeVore | 95. | D. P. Pope (Consultant) |
| 72. | C. R. Hubbard | 96. | E. R. Thompson (Consultant) |
| 73. | M. G. Jenkins | 97. | J. B. Wachtman, Jr. (Consultant) |

EXTERNAL DISTRIBUTION

- 98-110. Argonne National Laboratory, 9700 South Cass Avenue,
Building 212, Argonne, IL 60439
- A. Erdemir
G. Fenske
A. I. Michaels
F. A. Nichols (10)
111. Armco Steel Corporation, 703 Curtis Street, Middletown, OH 45043
W. Schumacher
112. Battelle Columbus Laboratories, 505 King Avenue, Columbus,
OH 43201
K. Dufrane
113. Carborundum Company, P.O. Box 832, Niagara Falls, NY 14302
M. Srinivasan
114. Caterpillar Tractor Company, 100 NE Adams, Peoria, IL 61629
D. I. Beihler
115. Cummins Engine Company, Box 3005, Columbus, IN 47202-3005
M. Naylor

116. Dartmouth College, Thayer School, Hanover, NH 03755
F. E. Kennedy, Jr.
117. Deere and Company Technology Center, 3300 River Drive, Moline,
IL 61265
P. Swanson
118. Eaton Corporation, 26201 Northwestern Highway, P.O. Box 766,
Southfield, MI 48037
J. Edler
119. Ferro Corporation, 661 Willet Road, Buffalo, NY 14218-9990
E. D. Porter
120. FMC Corporation, 1105 Coleman Avenue, Box 1201, San Jose,
CA 95108
J. Morrow
121. Ford Motor Company, Dearborn, MI 48121
G. M. Crosbie
122. Garrett Turbine Engine Company, P.O. Box 5217, Phoenix, AZ 85010
J. Boppart
123. General Motors, Detroit Diesel Allison, Romulus, MI 48174
N. Hakim
124. Georgia Institute of Technology, School of Mechanical
Engineering, Atlanta, GA 30332-0420
W. O. Winer
125. Greenleaf Corporation, 25019 Viking Street, Hayward, CA 94545
J. Greenleaf
126. IIT Research Institute, 10 West 35th Street, Chicago, IL 60616
V. Aronov
127. J. McCool, 250 Ridge Pike, Apt. 150B, Lafayette Hill, PA 19444
128. Kennemetal, P.O. Box 639, Greensburg, PA 15601
P. K. Mehrotra
129. Lanxide Corporation, Tralee Industrial Park, Newark, DE 19711
R. Dwivedi

130. Martin Marietta Laboratories, 1450 South Rolling Road, Baltimore,
MD 21227
A. C. Westwood
131. NASA Lewis Research Center, 21000 Brookpark Road, Cleveland,
OH 44135
T. Spalvins (23-2)
- 132-134. National Institute of Standards and Technology, Gaithersburg,
MD 20899
S. Hsu
S. Jahanmir
A. W. Ruff
135. National Materials Advisory Board, 2101 Constitution Avenue,
Washington, DC 20418
J. Lane
136. National Science Foundation, 1800 G Street, NW, Room 1110,
Washington, DC 20550
J. Larsen-Basse
137. Naval Research Lab, Washington, DC 20375
D. Lewis
138. Norton Company, Goddard Road, Northborough, MA 01532
J. Lucek
139. Office of Naval Research, 700 North Quincy Street, Arlington,
VA 22217-5000
L. H. Peebles (Code 1131)
140. Sunstrand Aviation, P.O. Box 7102, Rockford, IL 61125
J. Au
141. Technology Strategies Corporation, 10722 Shingle Oak Court,
Burke, VA 22015
E. Van Reuth
142. University of Rochester, Department of Mechanical Engineering,
Rochester, NY 14627
S. Burns
143. Vanderbilt University, Metallurgy Department, Box 1621,
Station B, Nashville, TN 37235
J. J. Wert

144-147. Department of Energy, ECUT Division, 1000 Independence Avenue,
SW, Washington, DC 20585

J. J. Eberhardt, CE-12

D. G. Mello, CE-12 (3)

148. Department of Energy, Oak Ridge Operations Office, P.O. Box 2001,
Oak Ridge, TN 37831-8600

Assistant Manager for Energy Research and Development

149-158. Department of Energy, Office of Scientific and Technical
Information, Office of Information Services, P.O. Box 62,
Oak Ridge, TN 37831

For distribution by microfiche as shown in DOE/TIC-4500,
Distribution Category UC-95 (Energy Conservation).